Pis'ma v ZhETF, vol. 102, iss. 1, pp. 23 – 29 

# The commensurability condition and fractional quantum Hall effect hierarchy in higher Landau levels

J. Jacak[1], L. Jacak

*Institute of Physics, Wrocław University of Technology, 50-370 Wrocław, Poland*

Submitted 3 February 2015
Resubmitted 27 April 2015

The odd structure of the fractional filling hierarchy, which is referred to as the fractional quantum Hall effect, is studied in higher Landau levels using the commensurability condition. The hierarchy of fillings that are derived in this manner is consistent with the experimental observations in the first three Landau levels. The relative poverty of the fractional structure in higher Landau levels compared with the lowest Landau level is explained using commensurability topological arguments. The commensurability criterion for correlated states specific for higher Landau levels (with $n \geq 1$), including also the paired states at half fillings of the spin-subbands of these levels, is formulated.

DOI: 10.7868/S0370274X15130056

**Introduction.** The rich structure of the fractional quantum Hall effect (FQHE) hierarchy in the lowest Landau level (LLL) [1] is in contrast to the scarce manifestation of a similar effect in the higher Landau levels (LLs) (with $n \geq 1$) [2]. This observation has been widely illustrated in many experiments using continuously enhanced precision on increasingly higher quality 2DEG samples [2–6] but has not been explained, although it has been confirmed by various numerical exact diagonalization studies on finite model systems [2]. In the LLL, the main hierarchy for the FQHE is predicted by the composite fermion (CF) model by mapping the FQHE at the actual fillings onto the integer Hall effect (IQHE) in higher LLs in the resultant magnetic field, which is screened by the mean field of CF flux-tubes [7, 8]. However, a similar approach failed to explain the fractional hierarchy of correlated states in higher LLs (the CF model does not explain also some ratios outside the main hierarchy in the LLL, e.g., 4/11, 4/5, 5/13, 5/7, 3/8, 3/10, ...). To address these drawbacks, one can use the topology-based approach for the FQHE hierarchy [9, 10], which may be applied to the lowest and higher LLs. The good correspondence of the predicted hierarchy using the topological approach with experimental observations supports the applicability of this method. Using the topological commensurability condition, one can identify the reason for the experimentally observed difference between the FQHE hierarchies in the lowest and higher LLs. Moreover, analysis of the fillings of higher LLs using the commensurability criterion provides information on the correlation type for particular ratios in the hierarchy in terms of the Halperin multicomponent generalization of the Laughlin function [11, 12].

**Commensurability condition in planar Hall systems.** The specific and exceptional topology of a 2D plane can be expressed in terms of the first homotopy group of the multiparticle configuration space, which is called the braid group (infinite in 2D) [13]. In the case of a 2D manifold (plane, locally sphere or torus) and in the presence of a strong magnetic field, the special structure of the related braid group emerges referred to the cyclotron braid subgroup [9, 10]. The one-dimensional unitary representations (1DURs) of braid groups, in particular, of the cyclotron braid subgroup, weigh the contributions of nonhomotopic classes of trajectories to the path integral [14, 15]. The braids (elements of braid groups) describe the particle exchanges along classical trajectories and can be referred to exchanges of variables $z_1, \dots, z_N$ of the multiparticle wave function $\Psi(z_1, \dots, z_N)$. This wave function must gain the phase shift according to the 1DUR of the braid, which describes the particular exchange of its variables [16, 17]. On the plane, the coordinate exchanges represented by braids are not permutations as in 3D. Distinct 1DURs of the appropriate 2D braid groups, in particular of the cyclotron braid subgroups at the quantizing magnetic field presence, coincide with the Laughlin statistics correlations [9].

The construction of the cyclotron braids is based on the interaction of particles that fixes the interparticle separation in the uniform planar system. The par-

[1] e-mail: janusz.jacak@pwr.wroc.pl

ticle interaction, the flat band that assures the identical kinetic energy of all particles, and the 2D topology constitute the necessary prerequisites to organize a collective FQH state. The cyclotron braid groups enable the identification of LL fillings at which the correlated multiparticle state of FQHE can be arranged by verifying the so-called commensurability condition. With the magnetic field in the 2D interacting system, the classical cyclotron orbits may or may not be commensurate with the interparticle separation. This commensurability admits the definition of the braid exchanges of particles (because the exchange trajectories must be cyclotronic orbits at magnetic field presence) which subsequently determines the statistics of a collective state using the unitary representations of the braid group. This method is general and enables the identification of FQHE correlations in the system for both the lowest and higher LLs. Higher LLs have different commensurability of orbits (because of higher kinetic energy) in comparison to the LLL, which explains why the FQHE structure is distinct in higher LLs compared with that in the LLL, as illustrated below.

In more formal terms, one can invoke the proof [15] that in the case of a not simply connected configuration space (such as a multiparticle configuration space), the path integral formula for the propagator $I_{a\to b}$ (which expresses the probability of the system transition form point $a$ to point $b$ in its configuration space) has the following form: $I_{a\to b} = \sum\limits_{\eta\in\pi_1} e^{i\alpha_\eta}\int d\lambda_\eta e^{iS[\lambda_\eta(a,b)]/\hbar}$, where $\pi_1$ denotes the full braid group, $S[\lambda_\eta(a,b)]$ is the action for the trajectory $\lambda_\eta(a,b)$, which links $a$ and $b$ with the added loop $\eta$ from $\pi_1$, $d\lambda_\eta$ is the measure in the homotopy sector $\eta$ of trajectories. The sum over nonhomotopic elements of $\pi_1$ reflects the impossibility of defining a uniform measure in the non-continuous path space divided into disjoint nonhomotopic fragments. The factors $e^{i\alpha_\eta}$ form 1DUR of the full braid group [15]. Different 1DURs correspond to different types of quantum particles that are related to the same classical particles. For $\dim M\geq 3$ ($M$ is the manifold on which the particles are located), there exist only two 1DURs of the full braid group because the full braid group in this case is the permutation group. These two 1DURs correspond to bosons ($\alpha_\eta=0$) and fermions ($\alpha_\eta=\pi$). Nevertheless, for $\dim M=2$, particularly for $M=R^2$, there exists an infinite number of full-braid group 1DURs with $\alpha_\eta=\alpha\in[0,2\pi)$, which correspond to anyons.

However, anyons do not exhaust all topological resources of the 2D plane. Another topological effect occurs in the presence of a perpendicular magnetic field that is sufficiently strong to shorten the cyclotron trajectories below the interparticle distances. The braid generators, $\sigma_i$, which are exchanges of neighboring particles along the cyclotron orbits, cannot be defined in this case because they are not sufficiently long for the exchanges. Nevertheless, it has been demonstrated [9, 18] that exclusively in the 2D case, the multi-loop exchanges can match the particles, and braid generators $\sigma_i$ must be substituted by $(\sigma_i)^q$, $q$ – *odd integer* (note that $(\sigma_i)^q=\sigma_i(\sigma_i)^{q-1}$, and $(\sigma_i)^{q-1}$ makes $\frac{q-1}{2}$ additional loops). The resulting "cyclotron braid subgroup", which is spanned by generators $(\sigma_i)^q$, $i=1,2,\ldots,N$, replaces the ordinary full braid group $\pi_1$ in the path integral. The 1DURs specific to the cyclotron braid subgroup reproduce the phase shift the same as given by the Laughlin correlations for the LLL filling factor $\nu=\frac{1}{q}$ [9, 10]. In this way the Laughlin statistics is obtained without a need to introduce CFs with auxiliary flux-tubes, which produces the required statistics by the Aharonov–Bohm effect [19].

Thus, the condition of commensurability of classical cyclotron orbits with the interparticle separation verifies whether the particle exchange trajectories along cyclotron orbits, which are required for the braid group definition in the presence of the magnetic field, can be implemented in the system or not. The details of this approach are described in Refs. [9] and [10]. For shorthand, let us refer here to the illustration in Fig. 1. In

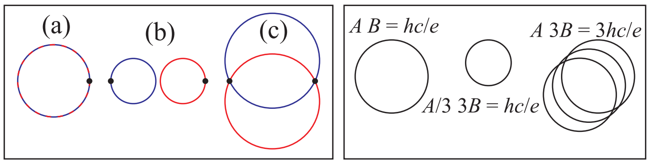


Fig. 1. Schematic illustration of the commensurability (left panel) of the cyclotron orbit with the interparticle separation: ideal fitting (a); overly short cyclotron radius, i.e., particles cannot be matched (b); overly large cyclotron radius, i.e., interparticle distances cannot be conserved (c). Schematic illustration of effective cyclotron orbit enhancement in 2D because of the multi-loop trajectory structure (right panel) (the third dimension is added for visual clarity)

the left panel, the picture displays the ideal fitting of the cyclotron orbit with a particle separation that allows for their interchange (a), overly short cyclotron orbits (b), and overly large cyclotron orbits (c). When the cyclotron orbits are overly short b) (e.g., for LLL filling factor $\nu=1/3$), in 2D system another possibility of exchanges occurs along multi-loop cyclotron orbits (cf. right panel of Fig. 1). The cyclotron orbit defines the surface $A$ (Fig. 1, right panel, left), which is accommodated to the particle velocity (being in average identical for all particles within the LL) and expressed by the magnetic field flux, i.e., $BA = \frac{hc}{e}$, in the LLL. This orbit $A$ fits to the sample surface per particle $\frac{S}{N}$, where $S$ is the sample area and $N$ is the number of particles, in the case of the completely filled LLL. In a $p$-fold-larger field than $B$ for a completely filled LLL, $pB$, the cyclotron orbit that is accommodated to the flux quantum (since the averaged particle velocity remains the same) is not sufficiently long compared to the interparticle separation $\frac{S}{N}$ (Fig. 1, right panel, central) for $p = 3$. However, if $p$-looped orbits are considered, then in the 2D case, the external flux $pBA$ for the field $pB$ must be shared between $p$ loops with the same surface $A$ (i.e., $BA$ for each loop). Thus, each loop that is accommodated to the flux quantum $\frac{hc}{e}$ has the orbit again with the surface $A$, which results in the total flux $pBA$ per particle (Fig. 1, right panel, right). The size of $A$ in (right panel, right) is equal to $A$ in (right panel, left), which indicates that the $p$-loop orbits fit the interparticle separation, which is defined by $A = \frac{S}{N}$, although the single-loop orbits (right panel, central) do not fit.

Let us emphasize that exclusively in 2D the surface of a planar orbit must be conserved; thus, a flux of the external field must be shared among all loops of the multi-loop orbit (in contrast to the 3D space, where each loop adds to the surface). This reduces the flux per loop and effectively increases the orbits. The multi-loop structure of classical trajectories, which are described by the cyclotron braid subgroup, enables the determination of quantum statistics, which satisfies Laughlin correlation requirements [9]. Thus, although the cyclotron orbit is a classical notion (as necessary for the braid group definition), its commensurability with the particle distribution allows us to discriminate the filling ratios for correlated states in any LL. The averaged velocity is greater in the higher LLs than in the LLL; thus, the cyclotron orbits increase their size in higher LLs, which causes there a distinct commensurability condition in comparison to the LLL (let us emphasize the classical character of the braids: the quantum orbits are not defined, similarly to as the particle velocity in Landau states, because $v_x$ and $v_y$ do not commute; the velocity can only be defined in LLs in average).

The commensurability condition for cyclotron orbits and interparticle separation allows us to recover the main FQHE hierarchy in the LLL (similar to the CF approach). The fraction of the external field flux $BS$ per the last loop of the $q$-looped orbit is $\phi = \frac{BS}{N} - (q-1)\frac{hc}{e}$ when the former loops take each flux quantum. If this residual flux fraction fits the fraction of flux per particle in certain higher $n$th LL, i.e., $\phi = \frac{hc}{(n+1)e}$, then one obtains the hierarchy,

$$\nu = \frac{l}{l(q-1) \pm 1}, \tag{1}$$

where $q$ is the number of loops (which must be odd to ensure particle interchanges along the braids $(\sigma_i)^q$) [9, 10] and $l = n + 1 = 1, 2, \ldots$ for the main line of the hierarchy[2)], $\pm$ in the denominator corresponds to consistent or opposite (figure-eight-shaped) orientation of the last loop with respect to the other loops [10].

**Commensurability and fractional filling hierarchy.** The single-particle energy in the $n$th LL has the form (including spin), $E_{n\uparrow(\downarrow)} = \hbar\omega_0\left(n + \frac{1}{2}\right) - (+)g\frac{1}{2}\hbar\omega_0$, where $\hbar\omega_0 = \frac{\hbar eB}{mc} = 2\mu_{\mathrm{B}}B$, $\mu_{\mathrm{B}} = \frac{e\hbar}{2mc}$ is the Bohr magneton, and $g$ is the giromagnetic factor. The degeneracy of each LL is identical and depends on the magnetic field, $N_0 = \frac{BS}{hc/e}$, where $BS$ is the total flux of the magnetic field $B$ through the sample surface $S$ and $\Phi_0 = \frac{hc}{e}$ is the quantum of the magnetic field flux. Let us assume that the sample (2D) surface $S$ is constant and the constant number of electrons in the system $N$ is maintained. Changing the magnetic field $B$ results in the variation of the LL degeneracy. If $B = B_0$, when $N_0 = N$, i.e., $N = \frac{B_0 S}{hc/e}$, then the filling factor $\nu = \frac{N}{N_0} = 1$, and we deal with the completely filled zeroth LL that exhibits a fully developed IQHE for spin-polarized electrons.

For higher magnitudes of the field, $B > B_0$, we have $N_0 > N$, i.e., $\nu = \frac{N}{N_0} < 1$. In this case, the cyclotron orbits are not sufficiently long to reach the neighboring particles; the multi-looped cyclotron orbits are needed to define the braid group and the appropriate statistics to organize a collective state. For $q$-loop orbits, the commensurability condition is, $q\frac{hc}{eB} = \frac{S}{N}$ which yields $\nu = \frac{N}{N_0} = \frac{SeB/qhc}{SeB/hc} = \frac{1}{q}$. Because $q$ must be odd to ensure that the corresponding exchange trajectories are braids [9], in this method, we obtain the main ratios for FQHE as $\frac{1}{q}$. According to Eq. (1), it can be generalized to the hierarchy $\nu = \frac{l}{l(q-1)\pm 1}$ (and symmetrically for subband holes, $\nu = 1 - \frac{l}{l(q-1)\pm 1}$).

For the fields $B < B_0$, when $2N_0 > N > N_0$, the subband $0\uparrow$ is completely filled with $N_0$ electrons, whereas the remaining electrons $N - N_0 < N_0$ must be located in the subband $0\downarrow$. The electrons $0\downarrow$ partially fill the subband $0\downarrow$, and their cyclotron orbits $\frac{S}{N_0}$ remain shorter than the particle separation $\frac{S}{N-N_0}$. Thus, the multi-loop trajectories are also required in this subband, which corresponds to the FQHE for the related

[2)] For "$-$" in the denominator in Eq. (1), $l = 2, \ldots$; moreover, for not-integer $l$, but for some characteristic fillings above the first subband, e.g., $l = 4/3$, $5/3$, $3/2$, one obtains from Eq. (1) the fractions $\nu$ outside the main CF line, $\nu = 4/11$, $4/5$, $5/13$, $5/7$, $3/8$, $3/10, \ldots$

electrons. For $q$-loop ($q$ is an odd integer to assure particle exchanges), $\nu = \frac{N}{N_0} = 1 + \frac{l}{l(q-1)\pm 1}$ and dually for holes in this subband, $\nu = 2 - \frac{l}{l(q-1)\pm 1}$. We see that in the subband $0\downarrow$, the filling hierarchy structure is repeated from the $0\uparrow$ subband.

If the magnetic field continues to decrease, i.e., $3N_0 > N > 2N_0$, then the subbands of LLL, i.e., $0\uparrow$ and $0\downarrow$, are completely filled with the IQHE for electrons in these subbands, whereas the remaining electrons, i.e., $N - 2N_0$, are located in the subband $1\uparrow$. Nevertheless, in the first LL, the cyclotron orbits are larger than in the LLL and equal to $\frac{3hc}{eB}$. Now, there are the following possibilities:

- $\frac{3hc}{eB} = \frac{3S}{N_0} = \frac{S}{N-2N_0}$. Thus, $\nu = \frac{N}{N_0} = \frac{7}{3}$, and in all subbands we deal with the single-loop orbits in a similar manner as in IQHE (although the subband $1\uparrow$ is not completely filled); this feature is a new Hall feature that is only possible for $n > 0$; the quantization of the transverse resistance $R_{xy}$ that is related to this fractional filling ratio of the first LL $\nu = \frac{hc}{eB} = \frac{7}{3}$ is similar to that for FQHE $\frac{h}{e^2\nu}$, but the correlations of the Laughlin type have the exponent $p = 1$, which displays single-loop braid exchanges similar to that in IQHE; this specific FQHE state is associated with single-loop cyclotron braids, in contrast to the multi-loop braided ordinary FQHE, which is typical for $n = 0$,
- the cyclotron orbit $\frac{3hc}{eB}$ in this band is not sufficiently long to match particles in this subband, $\frac{3hc}{eB} < \frac{S}{N-2N_0}$, which can occur for small $N - N_0$, i.e., for filling rates that are only close to the band edge; then, the multi-loop ($q$-loop, $q$ odd integer) trajectories are required, which results in the ordinary multi-loop-braid FQHE for these electrons: $q\frac{3hc}{eB} = \frac{S}{N-2N_0}$, and $\nu = 2 + \frac{1}{3q}$ $\Big($which can be developed to the hierarchy $\nu = 2 + \frac{l}{l\cdot 3(q-1)\pm 1}$ and for the holes in this subband $\nu = 3 - \frac{l}{l\cdot 3(q-1)\pm 1}\Big)$,
- the cyclotron orbit is twice in dimension of the interparticle separation: $\frac{3hc}{eB} = \frac{2S}{N-2N_0}$, then, $\nu = \frac{8}{3}$ enables the exchanges of every second particle; in this case, we address the single-loop braid ordering in all subbands, including the last one, which is incompletely filled with single-loop FQHE for $\nu = \frac{8}{3}$,
- the cyclotron orbit in the subband $1\uparrow$ fits three interparticle separations, i.e., $\frac{3hc}{eB} = \frac{3S}{N-2N_0}$ then $\nu = \frac{N}{N_0} = 3$, which corresponds to the completely filled first three subbands ($0\uparrow$, $0\downarrow$, and $1\uparrow$) with the IQHE correlation in all subbands.

When we continue to decrease the magnetic field $B$, we attain the region $4N_0 > N > 3N_0$, which corresponds to the partial filling of $1\downarrow$ subband. In this case, three antecedent subbands, $0\uparrow$, $0\downarrow$, and $1\uparrow$, are completely filled. We have $N - 3N_0 < N_0$ electrons in the subband $1\downarrow$. The cyclotron orbit $\frac{3hc}{eB}$ here may be overly small, equal or overly large compared with $\frac{S}{N-3N_0}$, which depends on $N$ and repeats the hierarchy form subband $1\uparrow$:

- overly short cyclotron orbits; this happens close to the band edge, at $\nu = \frac{N}{N_0} = 3 + \frac{1}{3q}$; in this case, the correlation in the $1\downarrow$ subband has the ordinary multi-loop FQHE character,
- if $\frac{3hc}{eB} = \frac{3S}{N_0} = \frac{S}{N-3N_0}$, then $\nu = \frac{10}{3}$, and the corresponding correlation in $1\downarrow$ has the single-loop character (single-loop FQHE),
- for $\frac{3hc}{eB} = \frac{3S}{N_0} = \frac{2S}{N-3N_0}$, i.e., for $\nu = \frac{N}{N_0} = \frac{11}{3}$, the commensurability holds for every second electron in the subband, which results also in the single-loop braid FQHE correlation for electrons in this subband,
- for $\frac{3hc}{eB} = \frac{3S}{N_0} = \frac{3S}{N-3N_0}$, we have $\nu = 4$ and the IQHE that corresponds to the commensurability of the cyclotron orbit with every third electron in the subband $1\downarrow$.

The symmetric ratios for holes in the subband $1\downarrow$ must also be considered.

The same scheme for commensurability repeats in the spin subbands in higher LLs, for which the cyclotron orbits are of increasing size, $\frac{(2n+1)hc}{eB}$, which further pushes the ordinary multi-loop FQHE toward the edges of the subbands, and $2n$ single-loop FQHE features appear in the central part of the subbands with $n > 0$ (e.g., for $2\uparrow$ subband at $\nu = 21/5$, $22/5$, $23/5$, $24/5$).

The corresponding filling ratios are summarized in Table for six first subbands of the LL structure (cf. Fig. 2), where the multi-loop FQHE is pushed toward the edges of spin subbands in higher LLs. The generalization of hierarchy (1) for the multi-loop FQHE in the $n$th LL has the form:

$$\nu = \begin{cases} 2n(+1) \pm \dfrac{l}{l(2n+1)(q-1)\pm 1}, & \text{for } \uparrow, \\ 2n+1(+1) \pm \dfrac{l}{l(2n+1)(q-1)\pm 1}, & \text{for } \downarrow, \end{cases} \quad (2)$$

where $n$ is the LL number and "(+1)−" for holes.

**Even-denominator fractions.** The commensurability conditions also enable the analysis of some special fractional fillings of LLs, which are expressed by

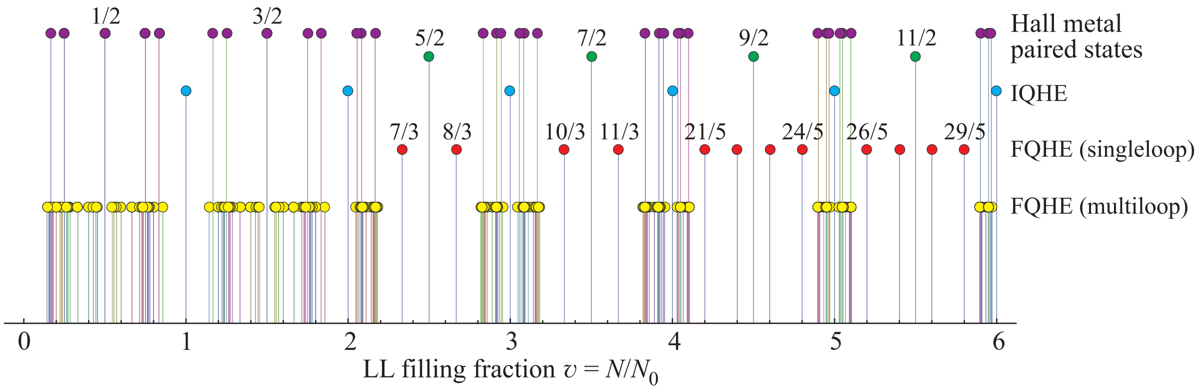


Fig. 2. Graphical presentation of the filling factors up to the sixth LL subband, which is selected using the commensurability condition: each spike represents the filling ratio for the possible correlated state; the shortest spikes correspond to the series of the multi-loop FQHE hierarchy given by (1) and (2), the medium spikes correspond to the single-loop-braid FQHE inside the bands with $n \geq 1$; the tallest spikes correspond to the paired states according to (3) and the Hall metal states according to (1) and (2) taken in the limit $l \to \infty$; the evolution of the FQHE filling hierarchy is visible with a growing number $n$ of the LL

**LL filling factors for FQHE (main) and other Hall features that are determined using the commensurability condition (*paired* indicates the condensate of electron pairs); for $l = 4/3, 5/3, 3/2, \ldots$, one can obtain in subband $0\uparrow$ all rates outside the main CF line (see footnote in p. 25) (note that $\pm$ in the denominators can be formally substituted by $l \to \pm l$)**

| LL subb. | FQHE (single-loop), IQHE, paired | FQHE (multi-loop) ($q$ – *odd*, $l = 1, 2, 3, \ldots$) | Hall metal |
|---|---|---|---|
| $0\uparrow$ | 1 | $\frac{l}{l(q-1)\pm1}$, $1-\frac{l}{l(q-1)\pm1}$ | $\frac{1}{q-1}$, $1-\frac{1}{q-1}$ |
| $0\downarrow$ | 2 | $1+\frac{l}{l(q-1)\pm1}$, $2-\frac{l}{l(q-1)\pm1}$ | $1+\frac{1}{q-1}$, $2-\frac{1}{q-1}$ |
| $1\uparrow$ | $\frac{7}{3}$, $\frac{8}{3}$, 3, $\left(\frac{5}{2}\right.$ paired$\left.\right)$ | $2+\frac{l}{3l(q-1)\pm1}$, $3-\frac{l}{3l(q-1)\pm1}$ | $2+\frac{1}{3(q-1)}$, $3-\frac{1}{3(q-1)}$ |
| $1\downarrow$ | $\frac{10}{3}$, $\frac{11}{3}$, 4 $\left(\frac{7}{2}\right.$ paired$\left.\right)$ | $3+\frac{l}{3l(q-1)\pm1}$, $4-\frac{l}{3l(q-1)\pm1}$ | $3+\frac{1}{3(q-1)}$, $4-\frac{1}{3(q-1)}$ |
| $2\uparrow$ | $\frac{21}{5}$, $\frac{22}{5}$, $\frac{23}{5}$, $\frac{24}{5}$, 5 $\left(\frac{9}{2}\right.$paired$\left.\right)$ | $4+\frac{l}{5l(q-1)\pm1}$, $5-\frac{l}{5l(q-1)\pm1}$ | $4+\frac{1}{5(q-1)}$, $5-\frac{1}{5(q-1)}$ |
| $2\downarrow$ | $\frac{26}{5}$, $\frac{27}{5}$, $\frac{28}{5}$, $\frac{29}{5}$, 6 $\left(\frac{11}{2}\right.$ paired$\left.\right)$ | $5+\frac{l}{5l(q-1)\pm1}$, $6-\frac{l}{5l(q-1)\pm1}$ | $5+\frac{1}{5(q-1)}$, $6-\frac{1}{5(q-1)}$ |

ratios with even denominators. The most prominent, $\nu = 5/2, 7/2, 9/2, 11/2, \ldots$, result from the special commensurability condition exclusively in $n > 0$ LLs, which corresponds to particle pairing,

$$\frac{(2n+1)hc}{eB} = \frac{\frac{2n+1}{2}S}{N - \begin{cases} 2nN_0, & \text{for } \uparrow \\ (2n+1)N_0, & \text{for } \downarrow \end{cases}}, \tag{3}$$

for the subbands $n\uparrow$ and $n\downarrow$, respectively. By pairing particles in the last subband, the ideal commensurability for the single-loop braid ordering of pairs can be achieved (by half reducing the denominator on the r.h.s. of Eq. (3), whereas the cyclotron orbits conserve their size for the pairs because the cyclotron radius scales as $\sim \frac{e}{m} = \frac{2e}{2m}$). This formula demonstrates that pairing may occur for $5/2$, $7/2$, $9/2, \ldots$ but not for $\nu = 1/2$ and $3/2$ from $n = 0$ spin subbands. In the spin subbands of the LLL, the cyclotron orbits are always shorter than the particle separation, which precludes pairing. The ratios $1/2$ and $3/2$ correspond to the Hall metal states, the condition for which can be obtained from the formulae (1) and (2), which are taken in the limit $l \to \infty$ (zero residual flux per the last loop). These properties are remarkably consistent with the experimental observations and numerical analysis of states that are proposed for related filling ratios, as recently summarized in Ref. [4].

**Comparison with experimental observations.** The odd structure of FQHE for $n = 1$, 2 compared to $n = 0$ LL is reported in Ref. [2]. The pronounced correlated state features at $\nu = 7/3$ and $8/3$ were observed in the magneto-transport experiment at ultra-low temperatures $\sim 15$ mK and for high mobility samples of GaAs/AlGaAs ($\mu \sim 11 \cdot 10^6\,\mathrm{cm}^2/\mathrm{V}\cdot\mathrm{s}$). They were interpreted as FQHE, which also accompanied such ordering at $\nu = 5/2$ (likely paired). It remains in contrast with the plethora of FQHE in the LLL. The relative absence of dense hierarchy of FQHE states in higher LLs coincides with the predictions based on the commensurability condition (Fig. 2). From this approach, it follows that the states at $7/3$, $8/3$ correspond to single-loop braid FQHE, which is not related with multi-loop tra-

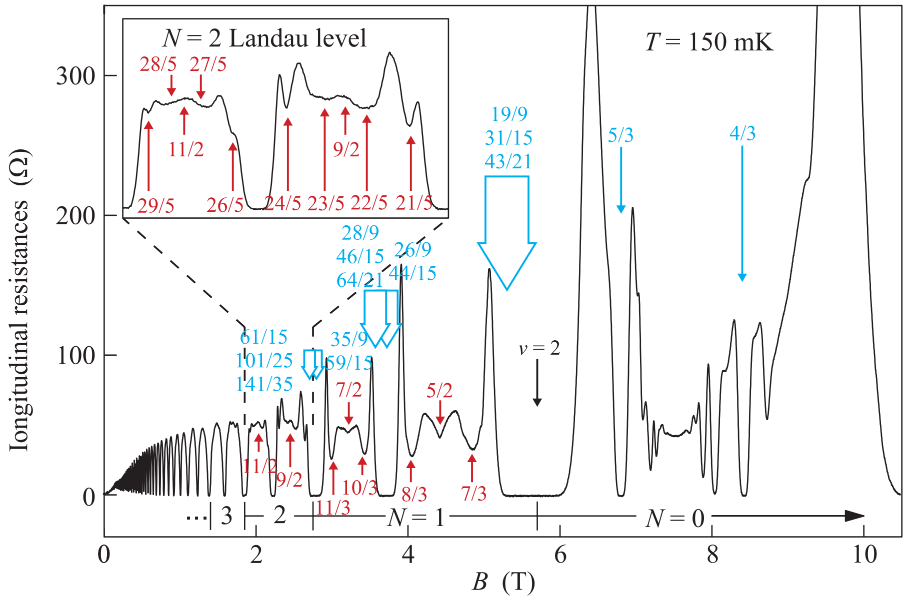


Fig. 3. (Color online) Resistivity measurements for a wide range of magnetic field corresponding to $n = 1, 2$ LLs in the high-mobility GaAs/AlGaAs heterostructure (after Ref. [2]); in red color there are indicated fractions for the FQHE-single-loop, and in blue color the fractions for the FQHE-multi-loop are shown, both of which are predicted using the commensurability condition (Fig. 2), in agreement with the experimentally observed features

jectories that are typical for the ordinary FQHE. Such states are numerically identified and observed in the experiment [3, 5]. Between these states, the 5/2 state is located regarded as FQHE for the filling fraction with an even denominator. The pairing expressed by various variants of Pfaffian function were considered for this state in exact diagonalization [4]. The fractional type of correlations for these states has been referred to the possibility of non-Abelian charges, which might be convenient for topological quantum information processing, as considered in Refs. [4, 5, 3]. Thus, the suggestion that states 7/3 and 8/3 are not of the multi-loop braid FQHE type but of the single-loop braid FQHE remarkably contributes to this discussion.

In $n = 2$ LL, the situation changes again [2], and two states with even denominators 9/2 and 11/2 occurred, which reveal, however, a strong anisotropy compared to the non-anisotropic states at 5/2 and 7/2. These states are accompanied by local minima, which perfectly fit to the single-loop FQHE states that are predicted using the commensurability criterion, $\{26/5, 27/5, 28/5, 29/5\}$, $\{21/5, 22/5, 23/5, 24/5\}$, $\{10/3, 11/3\}$, and $\{7/3, 8/3\}$, for single-loop-braid paired states, 11/2, 9/2, 7/2, and 5/2, respectively (cf. Table, Figs. 2 and 3).

Another feature predicted by the commensurability conditions, i.e., the location of series of the ordinary multi-loop-braid FQHE states in higher Landau LLs ($n \geq 1$) near the subband edges, also appears to be consistent with experimental observations, as marked in Fig. 3 by thick arrows. Densely lying FQH states near the IQH state are likely not distinguishable because of the measurement resolution and they may be mixed together resulting in a larger flattening of the main IQHE minimum, that is visible in the resistivity measurement (Fig. 3).

**Conclusion.** The topological braid group-based approach to FQHE is effective at recognizing the fractional fillings in the higher LLs and explaining the distinct structure of the FQHE in these levels compared with the LLL case. The reason for this latter property is identified in distinct size and distinct commensurability of the cyclotron orbits with the interparticle separation in various LLs. With a growing number of occupied LLs, the corresponding cyclotron orbit becomes larger because of the increase in kinetic energy in higher LLs and thus cyclotron orbits in higher LLs occur shorter than the interparticle separation only at relatively low densities of particles in correspoding LL subbands, near the subband edges. Thus, the ordinary multi-loop-braid FQHE is gradually pushed toward the edges of the subbands with an increasing LL number in opposition to the LLL, inside which the cyclotron orbits are never sufficiently long for particle interchanges (and multi-loop braids are always required in the LLL). In higher LLs, some new commensurability opportunities occur, which are impossible in the LLL. This new property resembles the commensurability in the completely filled subbands and corresponds to the single-loop orbits typical for IQHE but at some fractional fillings. Thus, these new features may be referred as to the single-loop-braid FQHE. The selected filling ratios using this type of commensurability are visible in the experiment similarly to the commensurability-predicted paired states at the centers of the subbands for $n \geq 1$. For the latter case, not affected by pairing cyclotron orbits are commensurate with twice-enhanced separation between pairs in the LLs with $n \geq 1$ but not in the LLL ($n = 0$), where an increase in separation (because of pairing) only worsens an opportunity to fit with an overly short cyclotron radius. Therefore, in the LLL at half fillings ($\nu = 1/2, 3/2$), we address the unpaired Hall metal, whereas for the half fillings of higher LLs, the pairing is necessary to fulfill the commensurability requirements. The Hall metal states in higher LLs occur, however, in association with the multi-loop fractional series near the band edges, if one takes the limit $l \to \infty$ in the generalized hierarchy (2), i.e., for zero residual flux fraction per the last loop of the multi-loop orbit.

Supported by NCN project # 2011/02/A/ST3/00116.


1. W. Pan, H.L. Störmer, D.C. Tsui, L.N. Pfeiffer, K.W. Baldwin, and K.W. West, Phys. Rev. Lett. **90**, 016801 (2003).
2. J.P. Eisenstein, M.P. Lilly, K.B. Cooper, L.N. Pfeiffer, and K.W. West, Physica E **6**, 29 (2000).
3. M. Dolev, Y. Gross, R. Sabo, I. Gurman, M. Heiblum, V. Umansky, and D. Mahalu, Phys. Rev. Lett. **107**, 036805 (2011).
4. R.L. Willett, Rep. Prog. Phys. **76**, 076501 (2013).
5. W. Pan, K.W. Baldwin, K.W. West, L.N. Pfeiffer, and D.C. Tsui, Phys. Rev. Lett. **108**, 216804 (2012).
6. J.S. Xia, W. Pan, C.L. Vicente, E.D. Adams, N.S. Sullivan, H.L. Störmer, D.C. Tsui, L.N. Pfeiffer, K.W. Baldwin, and K.W. West, Phys. Rev. Lett. **93**, 176809 (2004).
7. J.K. Jain, Phys. Rev. Lett. **63**, 199 (1989).
8. J.K. Jain, *Composite Fermions*, Cambridge UP, Cambridge (2007).
9. J. Jacak, I. Jóźwiak, and L. Jacak, Phys. Lett. A **374**, 346 (2009).
10. J. Jacak, R. Gonczarek, L. Jacak, and I. Jóźwiak, *Application of Braid Groups in 2D Hall System Physics: Composite Fermion structure*, World Scientific (2012).
11. B. I. Halperin, Helv. Phys. Acta **56**, 75 (1983).
12. M.O. Goerbig and N. Regnault, Phys. Rev. B **75**, 241405 (2007).
13. J. S. Birman, *Braids, Links and Mapping Class Groups*, Princeton UP, Princeton (1974).
14. Y. S. Wu, Phys. Rev. Lett. **52**, 2103 (1984).
15. M. G. Laidlaw and C. M. DeWitt, Phys. Rev. D **3**, 1375 (1971).
16. T. D. Imbo and E.C. G. Sudarshan, Phys. Rev. Lett. **60**, 481 (1988).
17. E.C.G. Sudarshan, T.D. Imbo, and T.R. Govindarajan, Phys. Lett. B **213**, 471 (1988).
18. J. Jacak and L. Jacak, Euorophysics Lett. **92**, 60002 (2010).
19. Y. Aharonov and D. Bohm, Phys. Rev. **115**, 485 (1959).